Journal of Integrated
SCIENCE & TECHNOLOGY

# Development and optimization of Hydrotropic Solid Dispersion of Dexlansoprazole using Central Composite Design approach

Ritu Gulia[1,2], Sukhbir Singh[3*], Sandeep Arora[4], Neelam Sharma[3]

*[1]Chitkara College of Pharmacy, Chitkara University, Punjab, India. [2]South Point College of Pharmacy, Sonepat, Haryana, India. [3]Department of Pharmaceutics, MM College of Pharmacy, Maharishi Markandeshwar (Deemed to be University), Mullana-Ambala, Haryana, India, [4]Amity Institute of Pharmacy, Amity University, Noida, Uttar Pradesh, India*

Received on: 15-Jan-2023, Accepted and Published on: 24-Mar-2023

## ABSTRACT

The objective of current research aims to enhance dissolution of dexlansoprazole (DLP) by organic solvent free and environment friendly approach through synthesis of hydrotropic solid dispersion (HSD) using water by solvent evaporation technique using sodium acetate and sodium alginate as hydrotropic agents. Central composite design was applied to analyze effect of drug: sodium alginate (X1) and drug: sodium acetate (X2) on response variables *i.e.* Q15 (Y1), Q45 (Y2), Q90 (Y3), t10% (Y4) and t50% (Y5) using Design Expert Software. This was revealed that quadratic model was superlative on account of insignificant p-value ($p$>0.05) for lack-of-fit analysis. The favourable values of optimized DLP-HSD were drug: sodium alginate (1: 2.78) and drug: sodium acetate (1: 4.41) which demonstrated highest desirability function (0.993). The study demonstrated that aqueous solubility and dissolution profile of DLP in DLP-HSD was enhanced 24-folds and 4.25-folds, respectively. This research conclusively manifested that hydrotropic solid dispersion hold enormous potential as organic solvent free and therefore, environmental friendly technique for enhancing solubility and dissolution of BCS class II drugs.

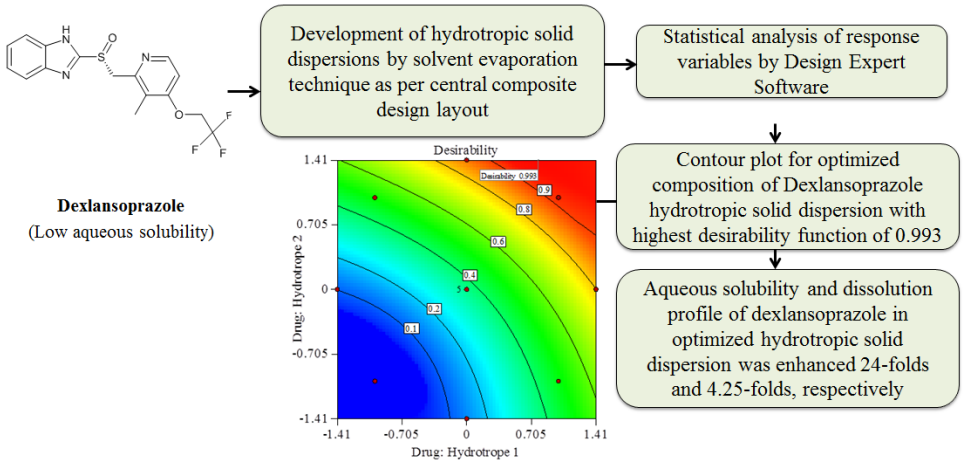


*Keywords: Dexlansoprazole, Crystalline, Hydrotropic Solid Dispersion, Solvent Evaporation Technique, Sodium Acetate, Sodium Alginate*

## INTRODUCTION

Dexlansoprazole (DLP) is an emerging new-generation proton-pump inhibitor for therapeutic of gastroesophageal reflux disease and erosive esophagitis symptoms.[1] The chemical formula of DLP is $C_{16}H_{14}F_3N_3O_2S$ with corresponding molecular weight of 369.36 Daltons. DLP belong to biopharmaceutical classification system II drug with log P and aqueous solubility of 2.84 and 0.250 mg/ml, respectively.[2–4] The chemical formula of Dexlansoprazole has been represented in Figure 1. The low aqueous solubility of DLP causes slow gastrointestinal drug absorption and limited oral bioavailability; therefore, augmentation in DLP solubility is required for amplifying its dissolution and bioavailability. In previous investigations of dexlansoprazole, researchers have developed superporous hydrogel tablets for gastroretentive drug delivery using sodium alginate, pectin and chitosan as hydrocolloids,[5] extended-release tablet using hydroxypropyl methyl cellulose (HPMC) phthalate and HPMC K100,[6] pH responsive nanoparticles using balangu seeds mucilage and Eudragit RS 100 for providing acid-protection as well as controlled drug delivery,[7] and double walled microspheres using sodium alginate, hydroxypropyl methyl cellulose E15 and xanthan gum.[8] In present research, an attempt has been made to enhance solubility of dexlansoprazole using hydrotropic solid dispersion (HSD) technique since previous researches have illustrated that HSD have

*Corresponding Author: Dr. Sukhbir Singh, MM College of Pharmacy, Maharishi Markandeshwar (Deemed to be University), Mullana-Ambala, Haryana, India.
Email: singh.sukhbir12@gmail.com

Cite as: *J. Integr. Sci. Technol., 2023, 11(4), 559. URN:NBN:sciencein.jist.2023.v11.559*

©Authors CC4-NC-ND, ScienceIN ISSN: 2321-4635
http://pubs.thesciencein.org/jist

tremendous potential in solubility enhancement of BCS class II drugs. [9–11]

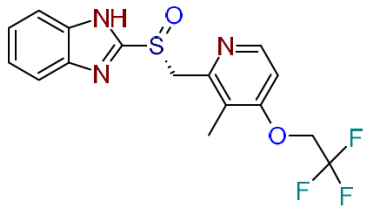


**Figure 1.** Chemical structure of Dexlansoprazole

The objective of this research was to enhance solubility and dissolution of dexlansoprazole by environment friendly approach which avoids involvement of organic solvents. Therefore, the hydrotropic solid dispersion of dexlansoprazole (DLP-HSD) was manufactured by solvent evaporation technique using sodium alginate and sodium acetate as hydrotropic agents and distilled water as solvent. The sodium alginate is biocompatible polymer [12] and sodium acetate has been approved as food additives by European Commission's food safety regulators.[13] The central composite design response surface methodology was applied to investigate influence of independent parameters on response variables like Q15 (Y1), Q45 (Y2), Q90 (Y3), $t_{10\%}$ (Y4) and $t_{50\%}$ (Y5) and to investigate optimized composition of DLP-HSD using Design Expert Software and further *in-vitro* evaluations of optimized formulation.

## MATERIALS AND METHODS

Dexlansoprazole was obtained from Alembic Pharmaceuticals Ltd, India. Sodium alginate and sodium acetate were bought from Loba Chemie Private Limited, India. The analytical grade chemicals were used during research.

### Experimental design

Thirteen batches of hydrotropic solid dispersion formulations were synthesized according to two-factor central composite design. The coded and actual values of independent and dependent parameters investigated during formulation development are depicted in Table 1. The design layout for 2-factor central composite design is shown in Table 2.

**Table 1.** Variables and their levels of central composite design explored during dexlansoprazole-loaded hydrotropic solid dispersion development

| Independent variables | Levels of variables | | | | |
|---|---|---|---|---|---|
| | **-1.41** | **-1** | **0** | **1** | **1.41** |
| Drug: Hydrotrope-1 (w/w) (X1) | 1:0.59 | 1:1 | 1:2 | 1:3 | 1:3.41 |
| Drug: Hydrotrope-2 (w/w) (X2) | 1:1.59 | 1:2 | 1:3 | 1:4 | 1:4.41 |
| **Dependent variables** | | | **Constraint** | | |
| Y1= Q15 (%) | | | Maximize | | |
| Y2= Q45 (%) | | | Maximize | | |
| Y3= Q90 (%) | | | Maximize | | |
| Y4= $t_{10\%}$ (Minutes) | | | Minimize | | |
| Y5= $t_{50}$% (Minutes) | | | Minimize | | |

### Production of Dexlansoprazole hydrotropic solid dispersion (DLP-HSD)

DLP-HSD formulations were manufactured by solvent evaporation technique using sodium alginate and sodium acetate as hydrotropic agent [9]. In Brief, sodium alginate (hydrotrope-1) and sodium acetate (hydrotrope-2) at specific drug: hydrotrope (as mentioned in Table 1) were dissolved in distilled water with subsequent addition of dexlansoprazole and continuous stirring at magnetic stirrer until semisolid mass production. Afterwards, semisolid product was stretched over watch glass and placed in oven at 60±5ºC till complete drying to yield DLP-HSD. Subsequently, DLP-HSD was screened through sieve # 30 and stored in desiccators.

**Table 2.** Design layout of 2-factor central composite design as per Design Expert software used for production of dexlansoprazole-loaded hydrotropic solid dispersion

| Batch | Independent variables | |
|---|---|---|
| | **X1** | **X2** |
| 1 | -1 | -1 |
| 2 | 1 | -1 |
| 3 | -1 | 1 |
| 4 | 1 | 1 |
| 5 | -1.41 | 0 |
| 6 | 1.41 | 0 |
| 7 | 0 | -1.41 |
| 8 | 0 | 1.41 |
| 9 | 0 | 0 |
| 10 | 0 | 0 |
| 11 | 0 | 0 |
| 12 | 0 | 0 |
| 13 | 0 | 0 |

X1: Drug: Hydrotrope-1; X2: Drug: Hydrotrope-2

### Evaluation of Dexlansoprazole hydrotropic solid dispersion

*In-vitro* drug release from DLP-HSD was performed using USP type II dissolution equipment (Electrolab Dissolution Tester, USP-TDT-06L) in phosphate buffer having pH 6.8 at 37±2ºC temperature conditions. Samples withdrawn at regular intervals were analyzed by ultraviolet spectrophotometer at 247 nm. Y1-Y5 was estimated from graph plotted between percentage cumulative drug release versus time (in minute) plot.[14–19]

### Selection of suitable design model for Y1-Y5 by Design-Expert Software

Y1-Y5 data investigation was executed to investigate sequential and lack-of-fit *p*-value, $R^2$, Adjusted-$R^2$ and Predicted-$R^2$ for choosing appropriate model among four different models *i.e.* linear, 2-factors-interaction (2-FI), quadratic and cubic model [20–22].

### Statistical analysis and model graphs investigation for Y1-Y5

Analysis of variance was executed to estimate *p*-value for chosen model and main, interaction and quadratic effect of independent parameters. The two- and three-dimensional graphs were

developed using model graph tool in design-expert software to show graphical manifestation of outcome of independent variables on Y1-Y5.[20,22–24]

**Optimization and Validation of DLP-HSD**

The composition of optimized DLP-HSD was found using predetermined standards of increasing Y1-Y3 while decreasing Y4-Y5 by numerical optimization using Design-Expert software.[25–27]

**Check point analysis**

The desirability function of design model was validated by manufacturing checkpoint batch of HSD which were further evaluated for Y1-Y5. The percentage bias was estimated using Eq. 1 for authenticating the optimization scheme.[28–30]

$$\% \text{ Bias } = \frac{\text{Predicted value} - \text{Experimental value}}{\text{Predicted value}} \times 100 \qquad \text{Eq. 1}$$

**Fourier transforms infrared spectroscopy (FTIR)**

FTIR spectrum of drug, sodium acetate, sodium alginate, physical mixture and optimized DLP-HSD were recorded on FTIR spectrophotometer (Shimadzu, Germany). The samples were blended with 1% KBr powder and compressed to self-supporting disks. Every spectrum was scanned in the analytical range of 400-4000 $cm^{-1}$.

**Percentage yield and solubility study of DLP-HSD**

The weight of DLP-HSD was accurately weighed using analytical balance and yield was calculated using Eq. 2 [15,31]. The saturation solubility of pure DLP and DLP-HSD in distilled water was performed using orbital shaker (Remi, India) at 37°C.[14,32]

$$\% \text{ Yield } = \frac{\text{Recovered weight of hydrotropic solid dispersion}}{\text{Initial weight of Dexlansoprazole+hydrotropes}} \times 100 \quad \text{Eq. 2}$$

***In-vitro* drug dissolution study and release kinetics of optimized DLP-HSD**

The composition of optimized DLP-HSD was found using predetermined standards of increasing Y1-Y3 whereas decreasing Y4-Y5 by numerical *In-vitro* drug release from optimized DLP-HSD was performed till 2 hours using USP dissolution paddle apparatus (Electrolab Dissolution Tester, USP-TDT-06L) in phosphate buffer, pH 6.8 under 100 rpm at 37±0.5°C (n=3). The samples taken at regular time periods of 15, 30, 45, 60, 90 and 120 minutes were analysed by spectrophotometer at 247 nm [33,34]. The drug release pattern from optimized DLS-SD was analysed by kinetic models viz. Zero order, First order, Higuchi, and Korsmeyer-Peppas on the basis of correlation coefficient ($r^2$) values.[35,36]

**Statistical Analysis**

The design optimization was executed by Design-Expert software while statistical analysis was performed using Bonferroni post-test using GraphPad Prism Software. The statistical difference was considered significant ($p < 0.05$).

## RESULTS AND DISCUSSION

**Selection of appropriate design model for Y1-Y5**

The difference between adjusted $r^2$ and predicted $r^2$ for Y1-Y5 for quadratic model was <0.2, *p*-value for lack-of-fit greater than 0.05 and sequential-*p*-value was <0.05 which illustrated suitability of quadratic model for analysis of Y1-Y5 (Table 3).

**Table 3.** Model summary statistics for estimation of best fit model for Y1-Y5 of DLP-HSD

| Source | Y | $R^2$ | Ad. $R^2$ | Pred. $R^2$ | LOF-*p* | Seq. *p*-value |
|---|---|---|---|---|---|---|
| Linear | Y1 | 0.8694 | 0.8433 | 0.7743 | 0.0101 | < 0.0001 |
| | Y2 | 0.9580 | 0.9496 | 0.9313 | 0.0039 | < 0.0001 |
| | Y3 | 0.8521 | 0.8225 | 0.7492 | 0.0002 | < 0.0001 |
| | Y4 | 0.7859 | 0.7430 | 0.6227 | 0.0623 | 0.0005 |
| | Y5 | 0.8741 | 0.8490 | 0.7701 | < 0.0001 | 0.0211 |
| 2FI | Y1 | 0.8994 | 0.8658 | 0.7677 | 0.0124 | 0.1361 |
| | Y2 | 0.9607 | 0.9476 | 0.9159 | 0.0033 | 0.4530 |
| | Y3 | 0.8769 | 0.8359 | 0.7446 | 0.0002 | 0.2104 |
| | Y4 | 0.8048 | 0.7397 | 0.5695 | 0.0561 | 0.3747 |
| | Y5 | 0.8893 | 0.8525 | 0.6490 | 0.2949 | 0.0202 |
| Quadratic | Y1 | 0.9891 | 0.9813 | 0.9529 | 0.3869 | 0.0004 |
| | Y2 | 0.9966 | 0.9942 | 0.9821 | 0.1748 | 0.0002 |
| | Y3 | 0.9961 | 0.9934 | 0.9777 | 0.0998 | < 0.0001 |
| | Y4 | 0.9497 | 0.9138 | 0.7731 | 0.3399 | 0.0087 |
| | Y5 | 0.9580 | 0.9280 | 0.7447 | 0.0603 | 0.0336 |
| Cubic | Y1 | 0.9944 | 0.9867 | 0.9885 | 0.8657 | 0.1842 |
| | Y2 | 0.9987 | 0.9968 | 0.9825 | 0.3959 | 0.0999 |
| | Y3 | 0.9980 | 0.9953 | 0.9328 | 0.1037 | 0.1829 |
| | Y4 | 0.9753 | 0.9407 | 0.8891 | 0.6803 | 0.1691 |
| | Y5 | 0.9815 | 0.9556 | 0.3033 | 0.1286 | 0.0790 |

**Statistical and Model Graph Analysis of Y1-Y5**

**Q15 (%) (Y1):** The main, interaction and quadratic effect of X1 and X2 over Q15 (%) was significant ($p < 0.05$) ($p < 0.05$) (Table 4). The polynomial Eq. 3 demonstrated that drug: hydrotrope 1 (X1) and drug: hydrotrope 2 (X2) have synergistic effect on Q15 (%). (b1= 7.81; b2 = 7.83) which has been illustrated in Figure 2a. This could be attributed to the solubilising characteristics of sodium alginate and sodium acetate which augmented the *in-vitro* drug dissolution.[37,38]. The previous research has also illustrated that HSD technique has potential effect in solubility enhancement of several other drugs like Gliclazide,[39] nimodipine,[40] and Rosuvastatin calcium.[41]

$$Y1 = 19.25 + 7.81X1 + 7.83\ X2 + 2.9\ X1X2 + 2.84\ X1^2 + 2.89\ X2^2 \qquad \text{Eq. 3}$$

**Table 4.** Analysis of variance for Y1 of DLP-HSD

| Source | Sum of Squares | Df | Mean Square | F-value | *p*-value |
|---|---|---|---|---|---|
| Model | 1108.94 | 5 | 221.79 | 126.75 | < 0.0001* |
| $X_1$ | 485.91 | 1 | 485.91 | 277.68 | < 0.0001* |
| $X_2$ | 488.88 | 1 | 488.88 | 279.38 | < 0.0001* |
| $X_1X_2$ | 33.58 | 1 | 33.58 | 19.19 | 0.0032* |
| $X_1^2$ | 55.60 | 1 | 55.60 | 31.78 | 0.0008* |
| $X_2^2$ | 57.79 | 1 | 57.79 | 33.03 | 0.0007* |
| Lack of fit | 6.07 | 3 | 2.02 | 1.31 | 0.3869 |

*$p < 0.05$

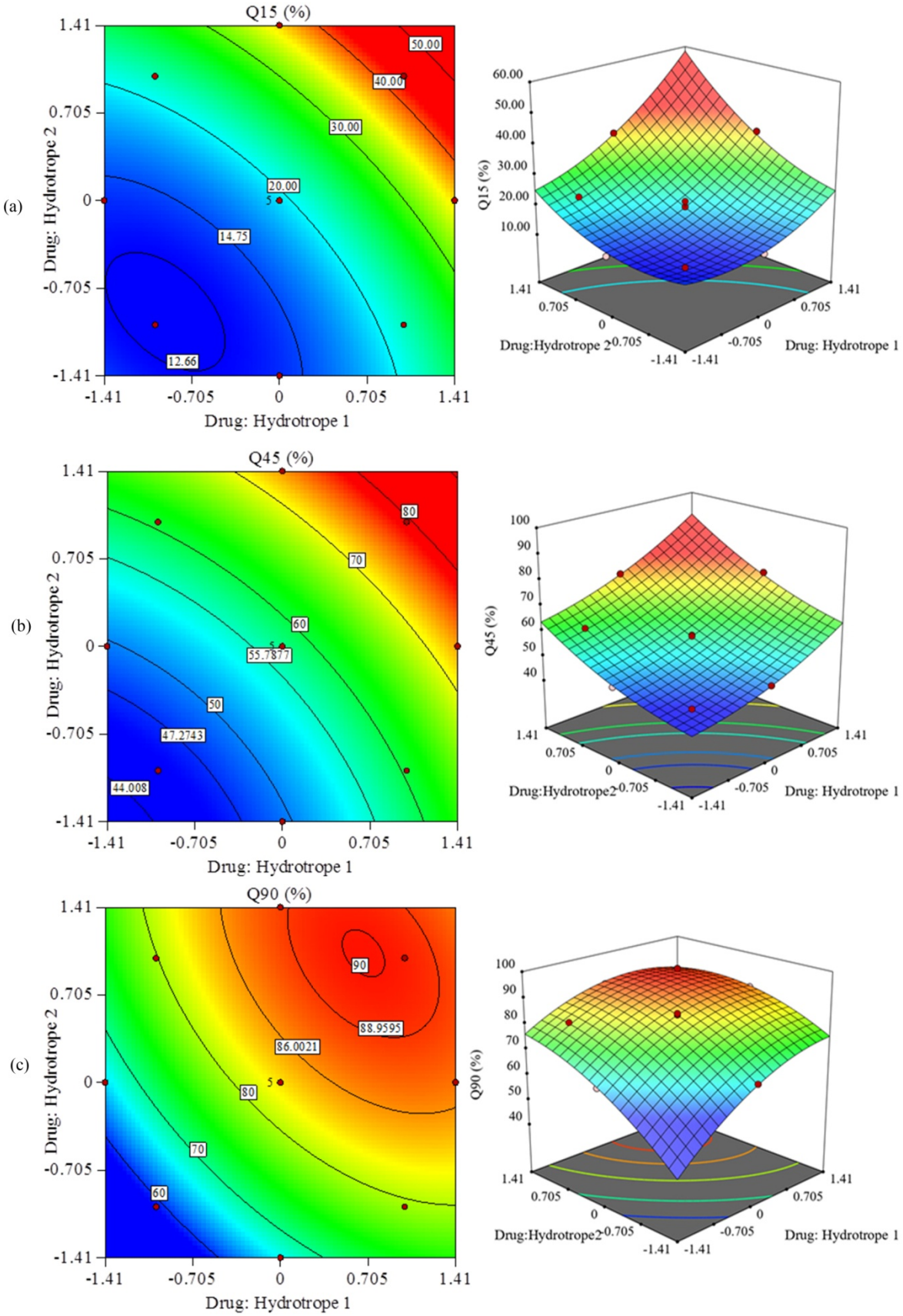


**Figure 2.** Contour plot and response surface plots for (a) Q15 (%) (b) Q45 (%) and (c) Q90 (%) of DLP-HSD

From polynomial equation 4, it has been revealed that drug: hydrotrope 1 (X1) and drug: hydrotrope 2 (X2) produced synergistic effect on Q45 (%) (b1= 8.43; b2 = 8.55) (Table 5) as represented graphically in Figure 2b. This could be attributed to solubilizing characteristics of sodium alginate and sodium acetate which augmented *in-vitro* drug dissolution.[40,42–44]

$$Y2 = 57.74 + 8.43X1 + 8.55\ X2 + 0.8975\ X1X2 + 1.88\ X1^2 + 1.87\ X2^2 \quad \text{Eq. 4}$$

**Table 5.** Analysis of variance for Y2 of DLP-HSD

| Source | Sum of Squares | Df | Mean Square | F-value | *p*-value |
|---|---|---|---|---|---|
| Model | 1195.45 | 5 | 239.09 | 413.95 | < 0.0001* |
| $X_1$ | 566.59 | 1 | 566.59 | 980.98 | < 0.0001* |
| $X_2$ | 582.54 | 1 | 582.54 | 1008.60 | < 0.0001* |
| $X_1X_2$ | 3.22 | 1 | 3.22 | 5.58 | 0.0502 |
| $X_1^2$ | 24.29 | 1 | 24.29 | 42.06 | 0.0003* |
| $X_2^2$ | 24.29 | 1 | 24.29 | 42.06 | 0.0003* |
| Lack of fit | 2.73 | 3 | 0.9100 | 2.77 | 0.1748 |

*$p < 0.05$

**Q90 (%) (Y3)**

From polynomial equation 5, it has been revealed that drug: hydrotrope 1 (X1) and drug: hydrotrope 2 (X2) produced synergistic effect on Q90 (%) (b1= 7.59; b2 = 7.89) (Table 6 and Figure 2c). This could be attributed to solubilizing characteristics of sodium alginate and sodium acetate which augmented the *in-vitro* drug dissolution.[41,45–47]

$$Y3 = 83.45 + 7.59X1 + 7.89\ X2 - 2.64\ X1X2 - 3.62\ X1^2 - 2.94\ X2^2 \quad \text{Eq. 5}$$

**Table 6.** Analysis of variance for Y3 of DLP-HSD

| Source | Sum of Squares | Df | Mean Square | F-value | *p*-value |
|---|---|---|---|---|---|
| Model | 1116.78 | 5 | 223.36 | 360.57 | < 0.0001* |
| $X_1$ | 459.35 | 1 | 459.35 | 741.54 | < 0.0001* |
| $X_2$ | 495.93 | 1 | 495.93 | 800.59 | < 0.0001* |
| $X_1X_2$ | 27.88 | 1 | 27.88 | 45.00 | 0.0003* |
| $X_1^2$ | 90.58 | 1 | 90.58 | 146.22 | < 0.0001* |
| $X_2^2$ | 59.61 | 1 | 59.61 | 96.23 | < 0.0001* |
| Lack of fit | 3.29 | 3 | 1.10 | 4.20 | 0.0998 |

*$p < 0.05$

**$t_{10\%}$ (Y4)**

The polynomial equation 6 illustrated that X1 and X2 have antagonistic effect on $t_{10\%}$ (b1= – 1.15; b2 = – 1.27) (Table 7). This confirmed that higher levels of sodium acetate and sodium alginate in HSD tend to reduce dissolution time (Figure 3a).[48–51]

$$Y4 = 10.6 – 1.15X1 - 1.27\ X2 + 0.375\ X1X2 – 0.2685\ X1^2 - 0.1715\ X2^2 \quad \text{Eq. 6}$$

**Table 7.** Analysis of variance for Y5 of DLP-HSD

| Source | Sum of Squares | Df | Mean Square | F-value | *p*-value |
|---|---|---|---|---|---|
| Model | 28.24 | 5 | 5.65 | 26.44 | 0.0002* |
| $X_1$ | 10.47 | 1 | 10.47 | 49.04 | 0.0002* |
| $X_2$ | 12.89 | 1 | 12.89 | 60.36 | 0.0001* |
| $X_1X_2$ | 0.5625 | 1 | 0.5625 | 2.63 | 0.1486 |
| $X_1^2$ | 0.4974 | 1 | 0.4974 | 2.33 | 0.1708 |
| $X_2^2$ | 4.11 | 1 | 4.11 | 19.22 | 0.0032* |
| Lack of fit | 3.29 | 3 | 1.10 | 4.20 | 0.0998 |

**$t_{50\%}$ (Y5)**

This was revealed from equation 7 that drug: hydrotrope 1 and drug: hydrotrope 2 produced antagonistic influence on $t_{50\%}$ (b1= – 4.71; b2 = – 4.78) (Table 8). This evidently proved that higher concentrations of sodium acetate and sodium alginate have a propensity for decreasing drug dissolution time (Figure 3b) [42,52–54].

$$Y5 = 41.40 – 4.71X1 - 4.78\ X2 + 1.25\ X1X2 – 1.08\ X1^2 - 1.83\ X2^2 \quad \text{Eq. 7}$$

**Table 8.** Analysis of variance for Y5 of DLP-HSD

| Source | Sum of Squares | Df | Mean Square | F-value | *p*-value |
|---|---|---|---|---|---|
| Model | 393.82 | 5 | 78.76 | 31.95 | 0.0001* |
| $X_1$ | 176.87 | 1 | 176.87 | 71.75 | < 0.0001* |
| $X_2$ | 182.47 | 1 | 182.47 | 74.02 | < 0.0001* |
| $X_1X_2$ | 6.25 | 1 | 6.25 | 2.54 | 0.1553 |
| $X_1^2$ | 8.04 | 1 | 8.04 | 3.26 | 0.1138 |
| $X_2^2$ | 23.21 | 1 | 23.21 | 9.42 | 0.0181* |
| Lack of fit | 14.06 | 3 | 4.69 | 5.86 | 0.0603 |

**Optimization and validation of DLP-HSD**

Optimal values of optimized DLP-HSD were found 1: 2.78 of drug: sodium alginate and 1: 4.41 of drug: sodium acetate with desirability (D-value) of 0.993 as proposed by Design-Expert shown in Figure 3c. The predicted values of Q15, Q45, Q90, $t_{10\%}$ and $t_{50\%}$ of optimized DLP-HSD were found 47.04%, 82.22%, 89.54%, 6.63 minutes and 28 minutes, respectively.[29,55]

**Check point analysis**

Optimized batch of DLP-HSD was synthesized and percentage bias for experimental and predicted Y1-Y5 was found < 5% which validated accuracy of predictive competence of designed model (Table 9).[56–58]

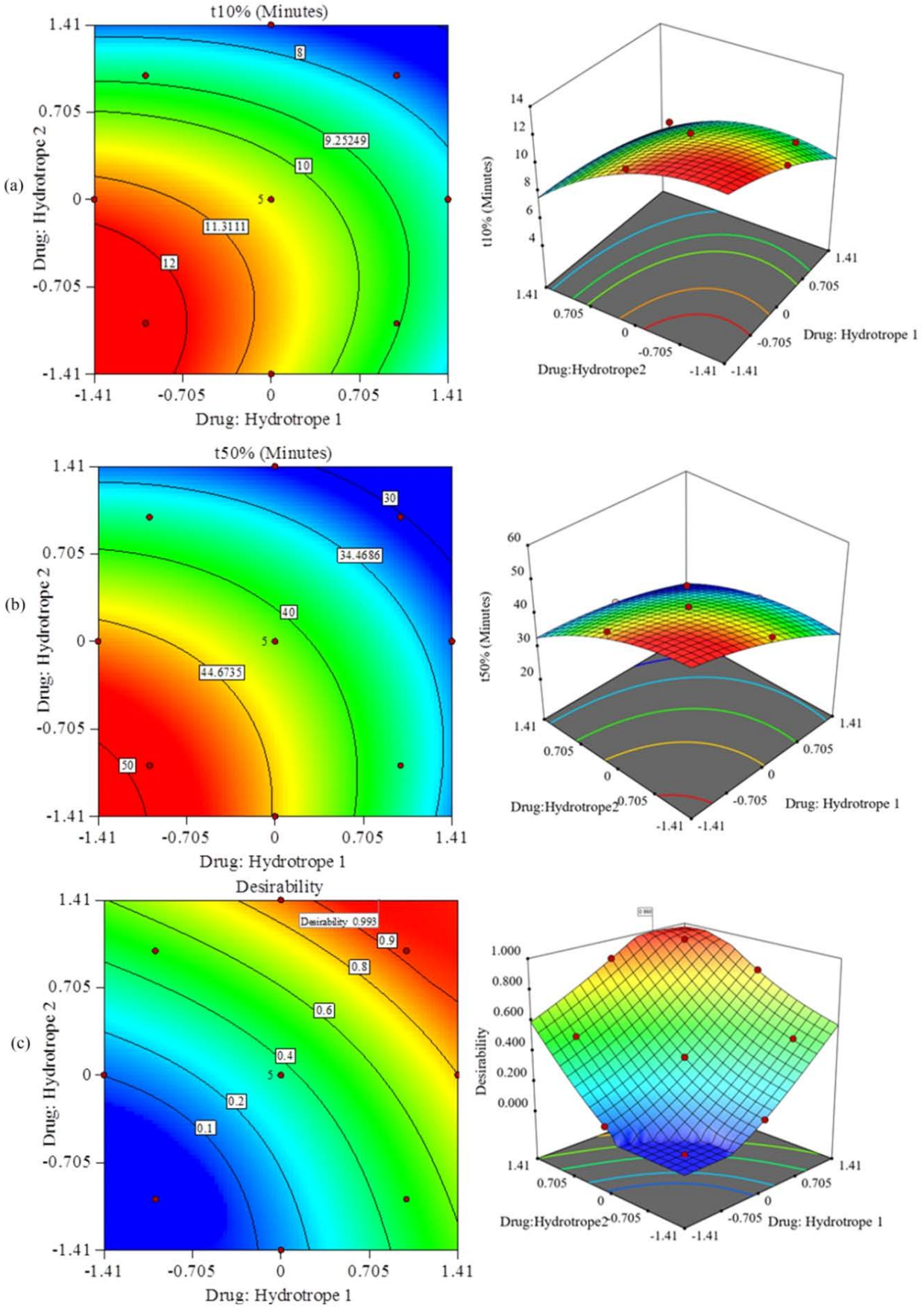


**Figure 3.** Contour plot and response surface plots for (a) $t_{10\%}$ (b) $t_{50\%}$ and (c) desirability function of DLP-HSD

**Table 9.** The perentage bias between experimental versus predicted values of Y1-Y5 for optimized DLP-HSD

| Response variables | Predicted value | Experimental value | Bias (%) |
|---|---|---|---|
| $Y_1$= Q15 (%) | 47.04 | 46.48 | 1.19 |
| $Y_2$= Q45 (%) | 82.22 | 81.15 | 1.30 |
| $Y_3$= Q90 (%) | 89.54 | 90.79 | 1.39 |
| $Y_4$= $t_{10\%}$ (Minutes) | 6.63 | 6.4 | 3.46 |
| $Y_5$= $t_{50\%}$ (Minutes) | 28 | 27 | 3.57 |

**Fourier transforms infrared spectroscopy**

The prominent peaks corresponding to drug and polymers were observed in FTIR spectra of drug-polymer blend (Figure 4). FTIR absorption peaks of DLS appeared at 3065, 1581, 1111, and 1034 $cm^{-1}$ for -NH- stretching vibration, carbon-carbon vibrations (s) in aromatic ring, the ether bond and the sulfinyl (S═O), respectively.[7,59] Sodium alginate exhibited absorption bands at 3553, 1631 and 1020 $cm^{-1}$ corresponding to –OH (stretching), asymmetric vibration (s) of -COO- and elongation of -C-O-, respectively.[60] Sodium acetate revealed stretching vibration at 1624 and 1408 $cm^{-1}$ of carbonyl groups, at 2926 $cm^{-1}$ of -CH vibration (s) of alkane and 3537 $cm^{-1}$ of –OH (s) of carboxylic acids.[61,62] FTIR spectra of DLP-HSD illustrated that neither additional peaks of DLP appeared nor any peak vanished in FTIR spectra of formulation which confirmed integration of drug within DLP-HSD.[63]

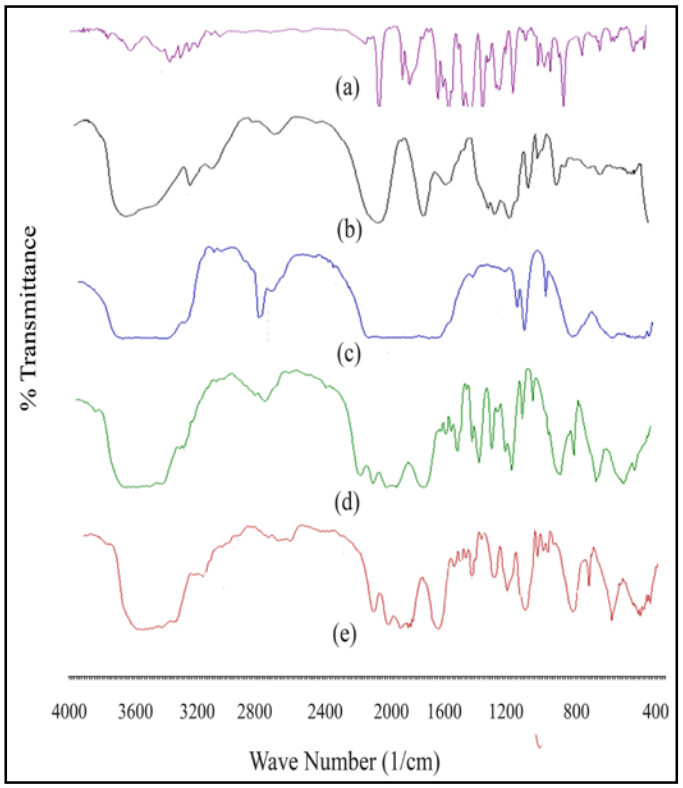


**Figure 4.** Fourier transform infrared spectroscopy of (a) dexlansoprazole (b) sodium acetate (c) sodium alginate (d) physical mixture, and (e) dexlansoprazole hydrotropic solid dispersion

**Percent yield and solubility of DLP-HSD**

The percentage yield of DLP-HSD was found to be 97.32 % ± 0.17. The aqueous solubility of DLP and DLP-HSD was 0.84 mg/ml and 20.16 mg/ml, respectively, which demonstrated that solubility of DLP was amplified 24-folds by synthesis of hydrotropic solid dispersion which could be due to highly hydrophilic characteristics of hydrotropes *i.e.* sodium alginate and sodium acetate [14,15,31,32].

***In-vitro* drug release profile and release kinetics for optimized DLP-HSD**

Dexlansoprazole, physical mixture and optimized DLP-HSD delivered cumulative drug release of 15.14%, 20.72% and 85.69% within 60 minutes, respectively and 22.17%, 37.18% and 94.28% within 120 minutes, respectively which demonstrated that % drug dissolution was amplified 4.25-fold which could be attributed to hydrophilic nature of hydrotropic solid dispersion (Figure 5A). DLP revealed low dissolution in phosphate buffer pH 6.8 which might be due to floating of drug on surface of dissolution medium. The improved dissolution rate was attributed to increase in drug wettability in presence of hydrotropic polymer and conversion of drug from crystalline to amorphous form.[64–66] The correlation coefficient ($r^2$) for drug release kinetic models from DLP-HSD was in sequence like higuchi (0.9474) > first-order (0.9454) > Korsmeyer-peppas (0.9109) > zero-order (0.6786). This revealed that drug release kinetics was best fitted in higuchi model which demonstrated that drug release from solid dispersion was dominated by fickian diffusion (Figure 5B).[67–69] This might be attributed to the increase in aqueous solubility of dexlansoprazole due to formation of the hydrophilic solid dispersion using water soluble sodium alginate and sodium acetate as hydrotropes.

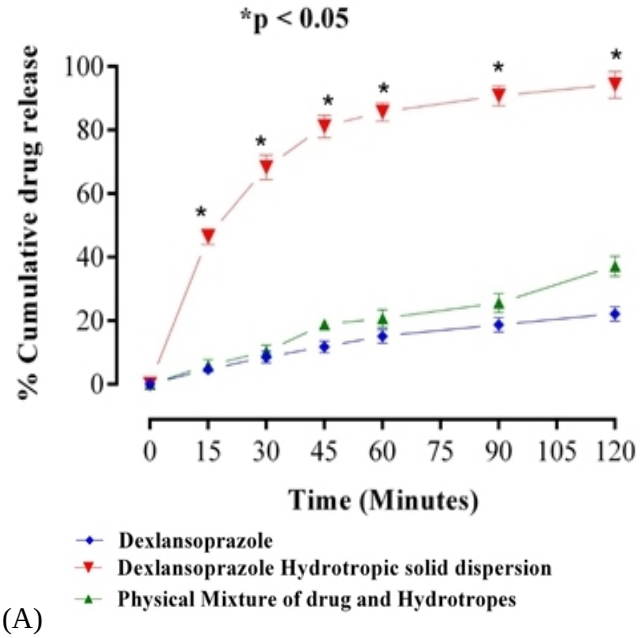


(A)

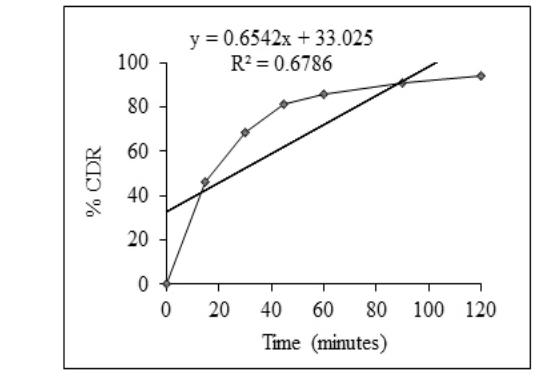


(a) Zero Order

(B)

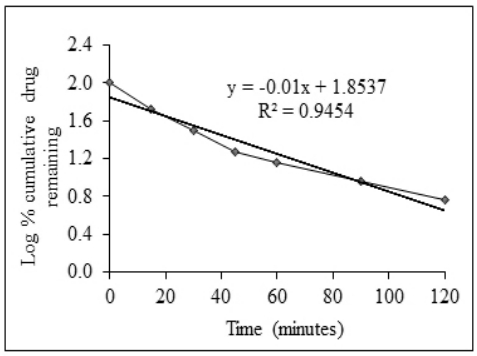


(b) First Order

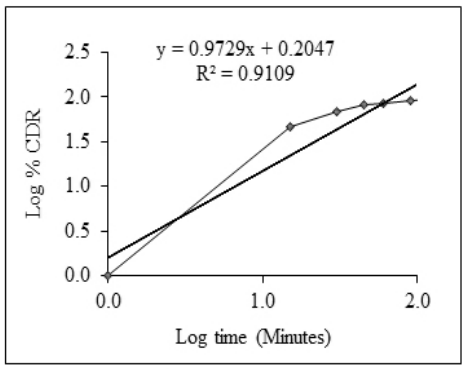


(c) Korsmeyer Peppas

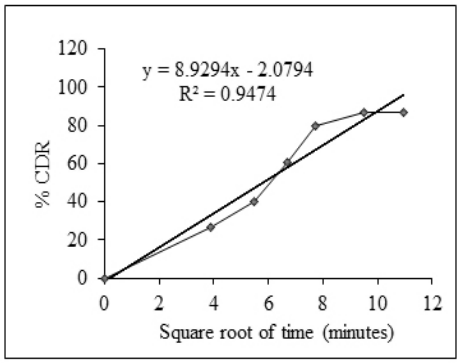


(d) Higuchi

**Figure 5.** (a) *In-vitro* drug release model from DLP, physical mixture and optimized DLP-HSD (values reported are mean ± SEM; n = 3) and (b) *In-vitro* drug release kinetic models for dexlansoprazole hydrotropic solid dispersion

## CONCLUSIONS

Hydrotropic solid dispersion of Dexlansoprazole was simply manufactured by environment friendly solvent-free strategy by solvent evaporation technique using sodium alginate and sodium citrate as hydrotropes. Central composite design analysed effect of drug: sodium alginate and drug: sodium acetate on dissolution parameters like Q15 (Y1), Q45 (Y2), Q90 (Y3), $t_{10\%}$ (Y4) and $t_{50\%}$ (Y5) of HSD. This has been disclosed that quadratic model was preeminent on account of $p > 0.05$ for lack-of-fit which indicated minimum signal/noise. The composition of optimized DLP-HSD was found 1: 2.78 (drug: sodium alginate) and 1: 4.41 (drug: sodium acetate) with desirability function of 0.993. The predicted response parameters for optimized DLP-HSD were Q15 (47.04%), Q45 (82.22%), Q90 (89.54%), $t_{10\%}$ (6.63 minutes) and $t_{50\%}$ (28 minutes) which were in close proximity with actual values. The study showed that synthesis of hydrotropic solid dispersion leads to increase in aqueous solubility and percentage drug dissolution of DLP by 24-folds and 4.25-folds, respectively. This research conclusively manifested that hydrotropic solid dispersion technology has enormous potential as organic solvent free approach in modifying the dissolution profile of BCS class II drugs in product development process.

## ACKNOWLEDGMENTS

The authors wish to thank Chitkara College of Pharmacy, Chitkara University, Punjab, India and Department of Pharmaceutics, MM College of Pharmacy, Maharishi Markandeshwar (Deemed to be University), Mullana-Ambala, Haryana, India for providing infrastructural support for this research study.

### CONFLICTS OF INTEREST

The authors do not have any conflicts of interest.

## REFERENCES

1. D.S. Strand, D. Kim, D.A. Peura. 25 years of proton pump inhibitors: a comprehensive review. *Gut Liver* **2017**, 11 (1), 27.
2. T. Hershcovici, L.K. Jha, R. Fass. Dexlansoprazole MR–a review. *Ann. Med.* **2011**, 43 (5), 366–374.
3. B.W. Behm, D.A. Peura. Dexlansoprazole MR for the management of gastroesophageal reflux disease. *Expert Rev. Gastroenterol. Hepatol.* **2011**, 5 (4), 439–445.
4. C.R. Emerson, N. Marzella. Dexlansoprazole: a proton pump inhibitor with a dual delayed-release system. *Clin. Ther.* **2010**, 32 (9), 1578–1596.
5. N.B. Pati, S. Velivela, V. Mayasa, V.R.M. Gupta. Gastroretentive superporous hydrogel tablets of dexlansoprazole. *Int. J. Pharm. Sci. Res.* **2016**, 7 (11), 4678.
6. S.S. Sharma, P.G. Bhutada. Formulation and evaluation of dexlansoprazole extended-release tablet. *GSC Biol. Pharm. Sci.* **2021**, 17 (3), 191–197.
7. A. Erum, U.R. Tulain, A. Maqsood, et al. Fabrication and comparative appraisal of natural and synthetic polymeric pH responsive nanoparticles for effective delivery of dexlansoprazole. *Polym. Bull.* **2022**, 1–17.
8. R. Vivek, N. Karra, B.R. Kamal. Formulation development and in-vitro evaluation of dexlansoprazole loaded double walled microspheres. *World J. Pharm. Sci.* **2021**, 5–10.
9. J.R. Madan, V.J. Kamate, R. Awasthi, K. Dua. Formulation, characterization and in-vitro evaluation of fast dissolving tablets containing gliclazide hydrotropic solid dispersions. *Recent Pat. Drug Deliv. Formul.* **2017**, 11 (2), 147–154.
10. R.K. Maheshwari, Y. Jagwani. Mixed hydrotropy: Novel science of solubility enhancement. *Indian J. Pharm. Sci.* **2011**, 73 (2), 179.

11. J.R. Madan, V.J. Kamate, K. Dua, R. Awasthi. Improving the solubility of nevirapine using a hydrotropy and mixed hydrotropy based solid dispersion approach. *Polym. Med.* **2017**, 47 (2), 83–90.
12. P.A.A. Borba, M. Pinotti, C.E.M. de Campos, B.R. Pezzini, H.K. Stulzer. Sodium alginate as a potential carrier in solid dispersion formulations to enhance dissolution rate and apparent water solubility of BCS II drugs. *Carbohydr. Polym.* **2016**, 137, 350–359.
13. A.N. Ngo, M.J.M. Ezoulin, J.B. Murowchick, A.D. Gounev, B.-B.C. Youan. Sodium acetate coated tenofovir-loaded chitosan nanoparticles for improved physico-chemical properties. *Pharm. Res.* **2016**, 33, 367–383.
14. N. Sharma, S. Singh. Central composite designed ezetimibe solid dispersion for dissolution enhancement: Synthesis and in vitro evaluation. *Ther. Deliv.* **2019**, 10 (10).
15. S. Singh, N. Sharma, G. Kaur. Central composite designed solid dispersion for dissolution enhancement of fluvastatin sodium by kneading technique. *Ther. Deliv.* **2020**, 11 (5).
16. N. Kanojia, S. Singh, N. Sharma. Development of Sustained Release Eudragit Based Matrix Tablet of Fluvastatin Sodium Microspheres. *Indian J. Pharm. Sci.* **2021**, 83 (6), 1229–1242.
17. B. Daravath, R.R. Tadikonda. Formulation and in vitro evaluation of flurbiprofen-polyethylene glycol 20000 solid dispersions. *J. Appl. Pharm. Sci.* **2014**, 4 (7), 76–81.
18. T.K. Panda, D. Das, L. Panigrahi. Formulation development of solid dispersions of bosentan using Gelucire 50/13 and Poloxamer 188. *J. Appl. Pharm. Sci.* **2016**, 6 (9), 27–33.
19. A.R. Shrivastava, B. Ursekar, C.J. Kapadia. Design, optimization, preparation and evaluation of dispersion granules of valsartan and formulation into tablets. *Curr. Drug Deliv.* **2009**, 6 (1), 28–37.
20. N. Sharma, S. Singh, S. Arora, J. Madan. Quality-by-design approach for development and optimization of nefopam hydrochloride loaded poly-(epsilon-caprolactone) and poly-3-hydroxybutyrate microspheres. *Int. J. Pharm. Sci. Res.* **2017**, 8 (12), 5111–5121.
21. J. Zhao, P. Gao, C. Mu, et al. Preparation and Evaluation of Novel Supersaturated Solid Dispersion of Magnolol. *AAPS PharmSciTech* **2022**, 23 (4), 1–17.
22. A. Mahajan, N. Surti, P. Patel, et al. Optimization of formulation and process variables using central composite design for the production of nevirapine spray dried solid dispersion. *Dry. Technol.* **2021**, 1–14.
23. X. Xue, G. Chen, X. Xu, et al. A combined utilization of Plasdone-S630 and HPMCAS-HF in ziprasidone hydrochloride solid dispersion by hot-melt extrusion to enhance the oral bioavailability and no food effect. *AAPS PharmSciTech* **2019**, 20 (1), 1–12.
24. A. Parikh, K. Kathawala, Y. Song, X.-F. Zhou, S. Garg. Curcumin-loaded self-nanomicellizing solid dispersion system: Part I: Development, optimization, characterization, and oral bioavailability. *Drug Deliv. Transl. Res.* **2018**, 8 (5), 1389–1405.
25. P. Chen, S. Lu, B. Pan, Y. Xu. Development, Optimization, and Pharmacokinetics Study of Bufalin/Nintedanib Co-loaded Modified Albumin Sub-microparticles Fabricated by Coaxial Electrostatic Spray Technology. *AAPS PharmSciTech* **2022**, 23 (1), 1–13.
26. M.F. Emam, A.A. El-Ashmawy, N.M. Mursi, L.H. Emara. Optimization of Meloxicam Solid Dispersion Formulations for Dissolution Enhancement and Storage Stability Using 33 Full Factorial Design Based on Response Surface Methodology. *AAPS PharmSciTech* **2022**, 23 (7), 1–21.
27. M. Kyaw Oo, U.K. Mandal, B. Chatterjee. Polymeric behavior evaluation of PVP K30-poloxamer binary carrier for solid dispersed nisoldipine by experimental design. *Pharm. Dev. Technol.* **2017**, 22 (1), 2–12.
28. F. A Maulvi, V. T Thakkar, T. G Soni, T. R Gandhi. Optimization of aceclofenac solid dispersion using Box-Behnken design: in-vitro and in-vivo evaluation. *Curr. Drug Deliv.* **2014**, 11 (3), 380–391.
29. A. Mahajan, N. Surti, P. Koladiya. Solid dispersion adsorbate technique for improved dissolution and flow properties of lurasidone hydrochloride: characterization using 32 factorial design. *Drug Dev. Ind. Pharm.* **2018**, 44 (3), 463–471.
30. K. Yuvaraja, S.K. Das, J. Khanam. Process optimization and characterization of carvedilol solid dispersion with hydroxypropyl-β-cyclodextrin and tartaric acid. *Korean J. Chem. Eng.* **2015**, 32 (1), 132–140.
31. J.N. Reginald-Opara, A. Attama, K. Ofokansi, C. Umeyor, F. Kenechukwu. Molecular interaction between glimepiride and Soluplus®-PEG 4000 hybrid based solid dispersions: Characterisation and anti-diabetic studies. *Int. J. Pharm.* **2015**, 496 (2), 741–750.
32. R.J. Boghra, P.C. Kothawade, V.S. Belgamwar, et al. Solubility, dissolution rate and bioavailability enhancement of irbesartan by solid dispersion technique. *Chem. Pharm. Bull.* **2011**, 59 (4), 438–441.
33. P.S. Yadav, V. Kumar, U.P. Singh, H.R. Bhat, B. Mazumder. Physicochemical characterization and in vitro dissolution studies of solid dispersions of ketoprofen with PVP K30 and d-mannitol. *Saudi Pharm. J.* **2013**, 21 (1), 77–84.
34. N. Zerrouk, C. Chemtob, P. Arnaud, S. Toscani, J. Dugue. In vitro and in vivo evaluation of carbamazepine-PEG 6000 solid dispersions. *Int. J. Pharm.* **2001**, 225 (1–2), 49–62.
35. S. Khan, H. Batchelor, P. Hanson, et al. Dissolution rate enhancement, in vitro evaluation and investigation of drug release kinetics of chloramphenicol and sulphamethoxazole solid dispersions. *Drug Dev. Ind. Pharm.* **2013**, 39 (5), 704–715.
36. J.S. Changdeo, M. Vinod, K.B. Shankar, C.A. Rajaram. Physicochemical characterization and solubility enhancement studies of allopurinol solid dispersions. *Brazilian J. Pharm. Sci.* **2011**, 47, 513–523.
37. A. Saharawat, N. Nainwal. Natural Plus Synthetic Hydrotropic Solubilization using Response Surface Methodology to Optimize the Solid Dispersion of Hydrochlorothiazide. *Comb. Chem. High Throughput Screen.* **2022**, 25 (2), 307–323.
38. S.D. Saoji, N.R. Rarokar, P.W. Dhore, et al. Phospholipid based colloidal nanocarriers for enhanced solubility and therapeutic efficacy of withanolides. *J. Drug Deliv. Sci. Technol.* **2022**, 70, 103251.
39. P. Nainwal, P. Sinha, A. Singh, D. Nanda, D.A. Jain. A comparative solubility enhancement study of rosuvastatin using solubilization techniques. **2011**.
40. N.J. Ibrahim, S.S. Smail, N.R. Hussein, T.A. Abdullah. Solubility enhancement of nimodipine using mixed hydrotropic solid dispersion technique. *Zanco J. Med. Sci. (Zanco J Med Sci)* **2020**, 24 (3), 386–394.
41. H. Abdullah Ali, H. Kamal Omer. Solubility Enhancement of a Poorly Water-Soluble Drug Using Hydrotropy and Mixed Hydrotropy-Based Solid Dispersion Techniques. *Adv. Pharmacol. Pharm. Sci.* **2022**, 2022.
42. G.P. Agrawal, R.K. Maheshwari, P. Mishra. Solubility enhancementofcefixime trihydrate by solid dispersions using hydrotropic solubilization technique and their characterization. *Brazilian J. Pharm. Sci.* **2022**, 58.
43. A.N. Ngo, D. Thomas, J. Murowchick, et al. Engineering fast dissolving sodium acetate mediated crystalline solid dispersion of docetaxel. *Int. J. Pharm.* **2018**, 545 (1–2), 329–341.
44. N.K. Yadav, T. Shukla, N. Upmanyu, S.P. Pandey, M.A. Khan. Novel application of mixed hydrotropic solubilization technique in the formulation and evaluation of solid dispersion of flupirtine maleate. *J. Drug Deliv. Ther.* **2018**, 8 (5), 481–488.
45. A. Kaushik, R.K. Jat. Solublity enhancement of miconazole by formulation of hydrotropic solid dispersions. *J. Drug Deliv. Ther.* **2017**, 7 (3), 117–126.
46. R. Kamble, S. Sharma, P. Mehta. Norfloxacin mixed solvency based solid dispersions: An in-vitro and in-vivo investigation. *J. Taibah Univ. Sci.* **2017**, 11 (3), 512–522.
47. D. Tripathi, S. Mishra, A.K. Rai, et al. Curcumin-loaded Hydrotropic Solid Dispersion Topical Gel Development and Evaluation: A Greener Approach Towards Transdermal Delivery of Drugs. *Curr. Green Chem.* **2022**, 9 (1), 26–39.
48. X. Liu, T. Wu, J. Yang, H. Li, W. Yang. Improved Bioavailability of Repaglinide by Utilizing Hydrotropy-Solid Dispersing Techniques and Prepared Its Dropping Pills. *J. Pharm. Innov.* **2022**, 1–9.
49. D. Tripathi, D.K. Sharma, J. Sahoo, S.K. Raman. Enhanced Solubility of Meloxicam with Sodium Benzoate Hydrotrope: Ecofriendly Approach for Improved Topical Drug Delivery. *INDIAN J. Pharm. Educ. Res.* **2022**, 56 (4), 1052–1062.
50. A.D. Khan, L. Singh. Various techniques of bioavailability enhancement: a review. *J. Drug Deliv. Ther.* **2016**, 6 (3), 34–41.

51. R. Kamble, S. Sharma, P. Mehta. Norfloxacin mixed solvency based solid dispersions. *Drugs* **2010**, 99, 3953–3965.
52. O. Jennotte, N. Koch, A. Lechanteur, B. Evrard. Development of amorphous solid dispersions of cannabidiol: Influence of the carrier, the hot-melt extrusion parameters and the use of a crystallization inhibitor. *J. Drug Deliv. Sci. Technol.* **2022**, 71, 103372.
53. M.R. Kazi, S. Gandhi, S. V Desai, R. Barse, V. Jagtap. Hydrotropy as Prominent Approach for Enhancement of Aqueous Solubility of Drugs. *J. Drug Deliv. Ther.* **2022**, 12 (4), 231–236.
54. F. Zhang, J. Mao, G. Tian, H. Jiang, Q. Jin. Preparation and Characterization of Furosemide Solid Dispersion with Enhanced Solubility and Bioavailability. *AAPS PharmSciTech* **2022**, 23 (1), 1–11.
55. A. Kumar Mahapatra, P. Narsimha Murthy, R. Kumari Patra, S. Pattnaik. Solubility enhancement of modafinil by complexation with β-cyclodextrin and hydroxypropyl β-cyclodextrin: a response surface modeling approach. *Drug Deliv. Lett.* **2013**, 3 (3), 210–219.
56. G. Ye, S. Wang, P.W.S. Heng, L. Chen, C. Wang. Development and optimization of solid dispersion containing pellets of itraconazole prepared by high shear pelletization. *Int. J. Pharm.* **2007**, 337 (1–2), 80–87.
57. N. Sun, X. Wei, B. Wu, et al. Enhanced dissolution of silymarin/polyvinylpyrrolidone solid dispersion pellets prepared by a one-step fluid-bed coating technique. *Powder Technol.* **2008**, 182 (1), 72–80.
58. S. Dhawan, R. Kapil, B. Singh. Formulation development and systematic optimization of solid lipid nanoparticles of quercetin for improved brain delivery. *J. Pharm. Pharmacol.* **2011**, 63 (3), 342–351.
59. Y.N. Kumar. Design and In Vitro Characterization of Dexlansoprazole Controlled Release Tablets. *Asian J. Pharm.* **2016**, 10 (04).
60. R. Pereira, A. Tojeira, D.C. Vaz, A. Mendes, P. Bártolo. Preparation and characterization of films based on alginate and aloe vera. *Int. J. Polym. Anal. Charact.* **2011**, 16 (7), 449–464.
61. H. Yang, X. Bao, H. Cui, T.Y. Lo, X. Chen. Optimization of supercooling, thermal conductivity, photothermal conversion, and phase change temperature of sodium acetate trihydrate for thermal energy storage applications. *Energy* **2022**, 124280.
62. C. Iacovita, R. Stiufiuc, T. Radu, et al. Polyethylene glycol-mediated synthesis of cubic iron oxide nanoparticles with high heating power. *Nanoscale Res. Lett.* **2015**, 10 (1), 1–16.
63. S. Sethia, E. Squillante. Solid dispersion of carbamazepine in PVP K30 by conventional solvent evaporation and supercritical methods. *Int. J. Pharm.* **2004**, 272 (1–2), 1–10.
64. N. Kolašinac, K. Kachrimanis, I. Homšek, et al. Solubility enhancement of desloratadine by solid dispersion in poloxamers. *Int. J. Pharm.* **2012**, 436 (1–2), 161–170.
65. R.H.K. Potluri, S. Bandari, R. Jukanti, P.R. Veerareddy. Solubility enhancement and physicochemical characterization of carvedilol solid dispersion with Gelucire 50/13. *Arch. Pharm. Res.* **2011**, 34 (1), 51–57.
66. M. Patel, A. Tekade, S. Gattani, S. Surana. Solubility enhancement of lovastatin by modified locust bean gum using solid dispersion techniques. *Aaps pharmscitech* **2008**, 9 (4), 1262–1269.
67. J.Y. Yu, J.A. Kim, H.J. Joung, J.A. Ko, H.J. Park. Preparation and characterization of curcumin solid dispersion using HPMC. *J. Food Sci.* **2020**, 85 (11), 3866–3873.
68. S. Solomon, J. Iqbal, A.B. Albadarin. Insights into the ameliorating ability of mesoporous silica in modulating drug release in ternary amorphous solid dispersion prepared by hot melt extrusion. *Eur. J. Pharm. Biopharm.* **2021**, 165, 244–258.
69. M. Skiba, M. Lahiani-Skiba, N. Milon, F. Bounoure, H. Fessi. Preparation and characterization of amorphous solid dispersions of nimesulide in cyclodextrin copolymers. *J. Nanosci. Nanotechnol.* **2014**, 14 (4), 2772–2779.